Available online at www.sciencedirect.com
ScienceDirect
Energy Procedia 48 (2014) 474 – 483
Energy Procedia

SHC 2013, International Conference on Solar Heating and Cooling for Buildings and Industry
September 23-25, 2013, Freiburg, Germany

Thermal performance of a hybrid BIPV-PCM: modeling, design and experimental investigation

Laura Aelenei[a]* , Ricardo Pereira[a], Helder Gonçalves[a], Andreas Athienitis[b]

[a] *Laboratório Nacional de Energia e Geologia (LNEG), Paço do Lumiar 22, 1649-038, Lisbon, Portugal*
[b] *Department of Building, Civil and Environmental Engineering, Concordia University, 1455 Maisonneuve W., Montreal, Quebec, Canada*

Abstract

In this paper, a BIPV-PCM installed in an office building façade is investigated to approach the practical application of PV-PCM. Based on an updated mathematical model, theoretical simulation has been conducted for BIPV-PCM in this case. Furthermore, field testing for this case has also been performed to validate the model, and then the simulated and experimental results are compared and found in considerably good agreement. The experiments have been conducted during the winter time, as the prototype has been installed in January 2013. The experimental and numerical results show a good agreement, the maximum electrical efficiency of this BIPV-PCM can reach 10% and the thermal one 12%.

Selection and peer review by the scientific conference committee of SHC 2013 under responsibility of PSE AG

Keywords: Building-integrated photovoltaic; Energy storage; Net Zero-Energy Buildings; Phase Change Material; Thermal modeling;

1. Introduction

Increasing energy consumption, shrinking resources and rising energy costs have significant impact on our standard of living for future generations. In this situation, the development of alternative, cost effective sources of energy for residential and non-residential buildings has to be a priority. Designing energy efficient and affordable solutions integrated in buildings dealing with summer and winter climate challenges represents a very ambitious

* Corresponding author. Tel.: +351 210 924 600
E-mail address: laura.aelenei@lneg.pt

Selection and peer review by the scientific conference committee of SHC 2013 under responsibility of PSE AG
doi:10.1016/j.egypro.2014.02.056

goal. In addition to this, in May 2010 it was published the recast of the Energy Performance of Buildings Directive which sets Zero Energy performance targets for all new buildings [1]. The integration of PV systems into buildings becomes an imperative in this context.

Nomenclature

Cp	Specific heat [J/(Kg.K)]
G	Total incident solar radiation on the plane of the collector per unit area [W/m^2]
h	Convective heat transfer coefficient per unit area [W/(m^2.K)]
h_r	Radiative heat transfer coefficient per unit area [W/(m^2.K)]
M	Thermal mass [Kg]
q_l	Latent heat flux when phase change occurs [W]
R	Thermal resistance [(m^2.K)/W]
T	Temperature [°C]
α	Solar absorptance
ε	Long-wave emissivity
σ	Stefan-Bolzmann constant

As is well known, zero-energy building design does not only mean the adoption of energy efficiency measures, but also the integration of renewable energy systems in order balance the building energy consumption. Integration of the photovoltaic systems in the roof or building façade is common in the existing zero-energy buildings. However, the integration of PVs and other renewable energy systems still constitute a challenge in building design, either from an architectural point of view, or from a recovery, storage and use of energy point of view. The present work reports preliminary results concerning the design of such a solution developed within the frame of a research project entitled "FRAME - Prefabricated systems for low energy buildings: design, modulation, prototyping and testing". The objective of the FRAME project is to investigate advanced technological prefabricated building façade modules which integrate photovoltaic panels (PV) and phase change materials (PCM). Their purpose is to improve the indoor thermal conditions and reduce building energy demand, through direct electricity generation, solar thermal contributions and energy storage in residential and non-residential buildings [2,3,4]. As is well known, only approximately 16% of the solar energy incident on a PV is converted to electricity, the remaining being absorbed and transformed into heat [5]. The component transformed into heat can cause overheating problems in the case of PV integrated systems [6]. Elevated operating temperatures, on the other hand, reduce the solar energy conversion efficiency of photovoltaic module. The study proposed in the FRAME project will follow two research lines: the improvement of the indoor thermal comfort, reducing at the same time the building energy demands, and the improvement of the efficiency of the photovoltaic system by limiting the temperature rise inside the system. These two objectives can be achieved by ventilating the air gap behind the PV module, the heat released in the conversion process from PV being successfully recovered for indoor heating (BIPV/T), and/or by using PCM for leveling the temperature difference between indoor and outdoor and a rapid stabilization of PV modules temperature (BIPV-PCM). The design of such system is a complex task that requires a detailed investigation (numerical an experimental) of the heat and mass transfer phenomena related to the prefabricated module. This paper addresses the preliminary investigation phase of this system which consists in the validation of the numerical model with the experimental results obtained during the heating period.

2. Numerical approach

The system was modelled using a 1-D dynamic simulation program with the real climatic data from the winter period measured on the building site. A control-volume based finite-difference scheme was used to solve the model equations developed under MATLAB/SIMULINK® with SIMSCAPE® library on a staggered grid. This software has a user-friendly interface and good flexibility. The SIMSCAPE® library permits a very dynamical simulation. In Fig. 1 (a) it can be observed the system configuration and the software models interface (b).

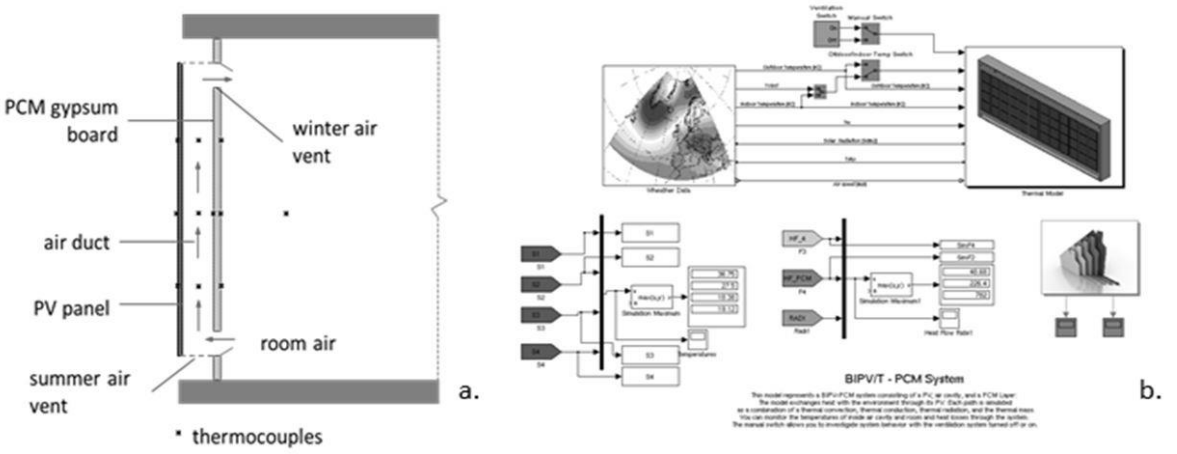

Fig. 1. (a) System configuration; (b) Software interface.

2.1. Thermal model

A heat transfer across the system can be considered as a set of nodes connected together by a thermal network, each with a temperature and capacitance. The numerical analysis considers the schematic thermal network of Fig. 2.

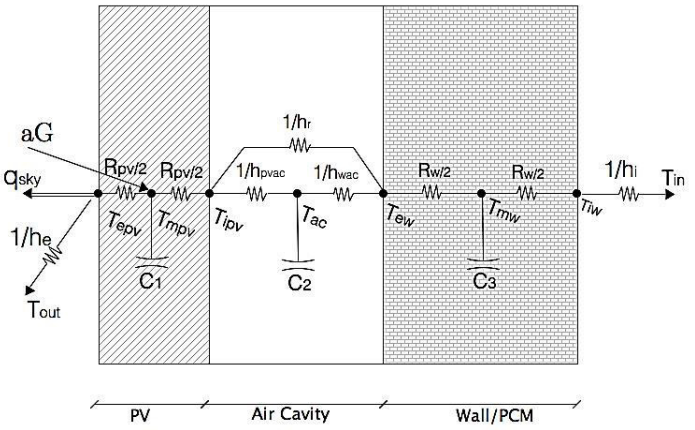

Fig. 2. Model studied – Thermal network.

2.1.1. Heat transfer across PV panel

For the PV panel layer, the energy balance can be obtained as shown in equation 1, where h_e represents convective heat transfer coefficient for exterior [7] and T_{sky} is the sky temperature employed to calculate the radiative heat losses to the exterior [8]. T_{out} and G represent the outside ambient temperature and solar radiation, respectively, which were experimentally deduced.

$$-\frac{\left(T_{epv}-T_{mpv}\right)}{R_{pv}/2}-\varepsilon_{pv}\cdot\sigma\cdot\left(T_{epv}^4-T_{sky}^4\right)-h_e\left(T_{epv}-T_{out}\right)=0 \quad (1)$$

$$M_{pv} \cdot Cp_{pv} \cdot \frac{dT_{mpv}}{dt} = \alpha_{pv} \cdot G + \frac{\left(T_{epv} - T_{mpv}\right)}{R_{pv}/2} - \frac{\left(T_{mpv} - T_{ipv}\right)}{R_{pv}/2} \quad (2)$$

2.1.2. Heat transfer within air gap

The heat transfer in the air gap is governed by natural convection although the radiation effects are considered assuming a view factor (FRpv-pcm) of 1 between planes [9]. The convective heat transfer coefficients inside air cavity are influenced by the operation mode of the system (open or closed vents). When vents are closed, the heat transfer coefficient assumes the Kalogirou [9] correlation for vertical collectors, whereas when the vents are open the convective heat transfer coefficient is based on Duffie and Beckman [8] correlation for natural ventilation described by Samar et al. [10]. The mean air velocity in gap is obtained by solving Bernoulli´s equation and assuming linear variation for air density and temperature as described in Kalogirou [9]. The energy balance within the air gap is described by the following equations:

$$\frac{\left(T_{mpv} - T_{ipv}\right)}{R_{pv}/2} - h_{pvac}\left(T_{ipv} - T_{ac}\right) - h_r\left(T_{ipv}^4 - T_{ew}^4\right) = 0 \quad (3)$$

$$M_{air} \cdot Cp_{air} \cdot \frac{dT_{ac}}{dt} = h_{pvac}\left(T_{ipv} - T_{ac}\right) + h_{wac}\left(T_{ac} - T_{ew}\right) \quad (4)$$

$$h_r\left(T_{ipv}^4 - T_{ew}^4\right) - h_{wac}\left(T_{ac} - T_{ew}\right) - \frac{\left(T_{ew} - T_{mw}\right)}{R_w/2} = 0 \quad (5)$$

2.1.3. Heat transfer across PCM gypsum board

The energy balance for the PCM gypsum board can be obtained from equations 6 and 7 where h_i is the interior heat transfer coefficient based on the Santos et al, [11] and q_i is based on the Athienitis [12] approach for PCM model.

$$M_w \cdot Cp_w \cdot \frac{dT_{mw}}{dt} = \frac{\left(T_{ew} - T_{mw}\right)}{R_w/2} - \frac{\left(T_{mw} - T_{iw}\right)}{R_w/2} + q_l \quad (6)$$

$$\frac{\left(T_{mw} - T_{iw}\right)}{R_w/2} - h_i\left(T_{iw} - T_{in}\right) = 0 \quad (7)$$

3. Experimental approach

The BIPV-PCM prototype has been installed on the main façade of SolarXXI office building in Lisbon in January 2013 and tested under real conditions (Fig. 3). The 0.73 × 1.75 m prototype consists of an outer layer (PV panel) and an inner layer (gypsum wallboard incorporating PCM, Alba®balance type).

When the BIPV-PCM prototype is exposed to sunlight during the day, the PV panels absorb solar radiation and generate heat during the conversion process which is then stored by the PCM gypsum board. During the night, the melted PCM solidifies and delivers the heat back keeping the system warm for a longer period of time. The BIPV-PCM system is designed to be integrated within the building envelope and store the thermal energy directly into the building wall structure. The external and internal frame of the prototype is equipped with a ventilation system that can provide, if necessary, indoor or outdoor ambient air into the gap. The air flow can be controlled by opening or

closing the slot openings. The inner layer (plaster PCM board) is movable in order to vary the air gap depth for a more detailed evaluation of its influence on the overall system behavior.

Fig. 3. Views of the prototype installed on the SolarXXI main façade.

The inner PCM gypsum board is made of Alba®balance plasterboards and the outer layer uses PV polycrystalline modules with a peak power, Pmax, of about 120 Wp. The air gap formed between inner and outer layer is approximately 10 cm in depth. The properties of each layer are resumed in the Table 1.

Table 1. Materials properties.

Material	Thickness *m* *L*	Conductivity *W/m.K* *K*	Specific Heat *J/Kg.K* C_p	Density Kg/m^3 ρ	Other Properties		
					Short Circuit Current *A* I_{SC}	Open Circuit Voltage *V* V_{OC}	
PV	0,0038	148	677	2330	7,7	21,8	
					Kinematic viscosity m^2/s ν	Expansion Coefficient *1/K* β	
Air	0,01	0,0257	1007	1,205	$15{,}11 \times 10^{-6}$	$3{,}43 \times 10^{-3}$	
					Latent Heat *J/kg* *L*	Start Freezing ◦*C* T_1	Ends Freezing ◦*C* T_2
PCM	0,025	0,33	1132	1000	12000	18	23

2.2 Experimental setup

In order to evaluate the thermal behavior of the system the installed prototype was fully monitored by sensors mounted on all surfaces, in the air gap and indoors and outdoors. Four thermal sensors type PT 100 (2 mm × 2,3 mm) were used for measuring the surface temperature of each layer of the prototype, one for each surface. To obtain a more complete assessment of the surface temperatures, another four Self Adhesive Patch sensors have been applied, one for each surface. Heat flux measurements have been performed using Hukseflux sensors of HFP01-05 type. The air gap temperature was monitored with three PT100 sensors placed at three different levels, as it can be observed in Fig. 4. The exterior and interior ambient temperatures were measured using PT100 sensors and the solar global irradiation was measured using a Hukseflux SR11 sensor. The sensors location is listed in Table 2 and shown in the cross-section set-up in Fig. 4.

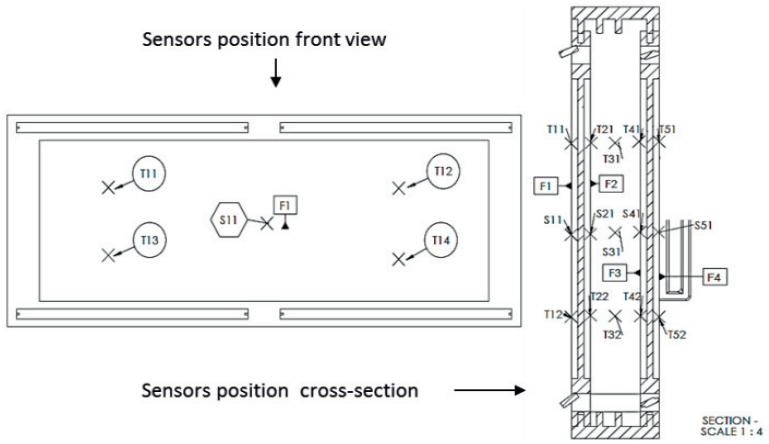

Fig. 4. Cross-section set-up and sensors positions.

Table 2. List of sensors and their individual location.

PCM surface facing room	PCM surface facing air gap	Air gap between PCM and PV	PV facing air gap	PV outside
PT100 2x2,3mm	PT100 2x2,3mm	PT100 2x2,3mm	PT100 2x2,3mm	PT100 2x2,3mm
T51	T41	T31	T21	T11
T52	T42	T32	T22	T12
T53	T43	T33	T24	T13
T54	T44	T34	T25	T14
Patch PT100	Patch PT100		Patch PT100	Patch PT100
S51	S41		S21	S11
Hukseflux HFP01-05	Hukseflux HFP01-05		Hukseflux HFP01-05	
F5	F4		F2	

2.3 *Measurement campaign*

This paper reports the results obtained during the heating period in two representative days of winter time.

Table 3. Experimental values.

Time	I (W/m^2)	Tout (◦C)	PV int (◦C)	Air (◦C)	PCM ext (◦C)	PCM int (◦C)	Tin (◦C)
10:00	694,2	8,4	43,6	35,61	24,38	20,81	19,0
11:00	814,6	9,1	52,25	43,39	33,02	27,70	20,7
12:00	866,3	10,5	54,51	47,57	37,91	31,57	20,8
13:00	848,6	10,2	55,75	49,14	40,15	32,95	20,7
14:00	784,4	12,0	56,58	49,38	40,63	33,19	20,7
15:00	680,7	13,0	51,85	44,49	38,01	30,82	20,2
16:00	492,9	12,0	41,91	36,61	32,90	28,49	20,5
17:00	21,9	10,3	18,05	21,98	26,45	25,71	20,6

The first campaign of experimental tests was carried out over a 2-day period, from 24th to 25th of February 2013, which was characterized by maximum solar radiation values around 900W/m^2 and outdoor ambient temperatures ranging from 4ºC to 12ºC. The corresponding external ambient conditions, together with the measured surface temperatures in cross-section for one representative day are summarized in Table 3 and shown in Fig. 5.

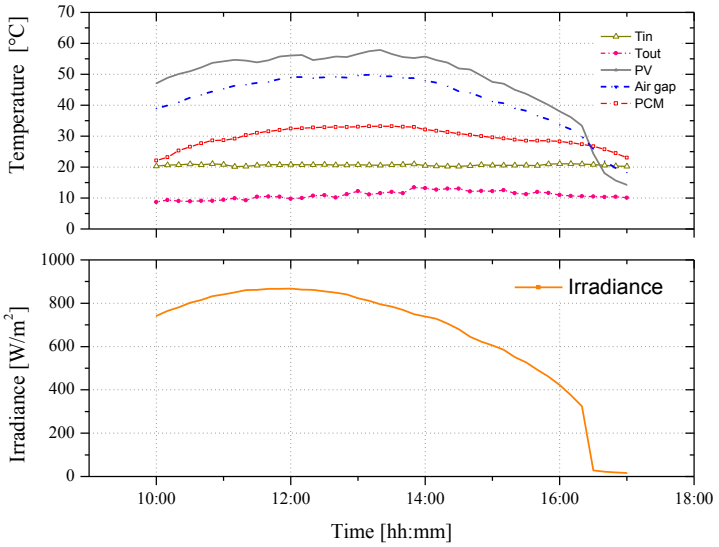

Fig. 5. External ambient conditions (Irradiation and external temperature)

4. Results

4.1. Validation of numerical model

The numerical model above was validated against experimental data collected over the 2-day period. Throughout the night the vents remained closed, while during the day the vents were opened. The time step used in the simulations corresponds to that used by the data acquisition system which is 10 minutes. The initial conditions in the numerical model were set according to the corresponding measured values. As the SolarXXI building, where the system was tested, is a building with daytime occupation (office), only the results for the period of time from 10 a.m. to 5 p.m. are presented. The numerical versus experimental results of the thermal behavior of the BIPV-PCM in terms of internal surface temperatures of the photovoltaic module (PV int), PCM (PCM int) and temperature of the air in the gap (Air) are shown in Fig. 6.

The comparison between experimental and numerical results shows relatively good agreement. The maximum difference between numerical and experimental results in the first and second day is around 3,5 to 4,0 ºC and 2,5-3ºC, respectively. A likely explanation of these differences is that they occur when the vents are opened and air begins to flow through the gap driven by the pressure differences which are also induced by the wind action on building surface which was not measured. The numerical model was not able to describe reliably the PV temperature surface changes. This dynamic behavior is observed also in the case of the air gap temperature. However, the differences in PCM gypsum board temperatures are lower.

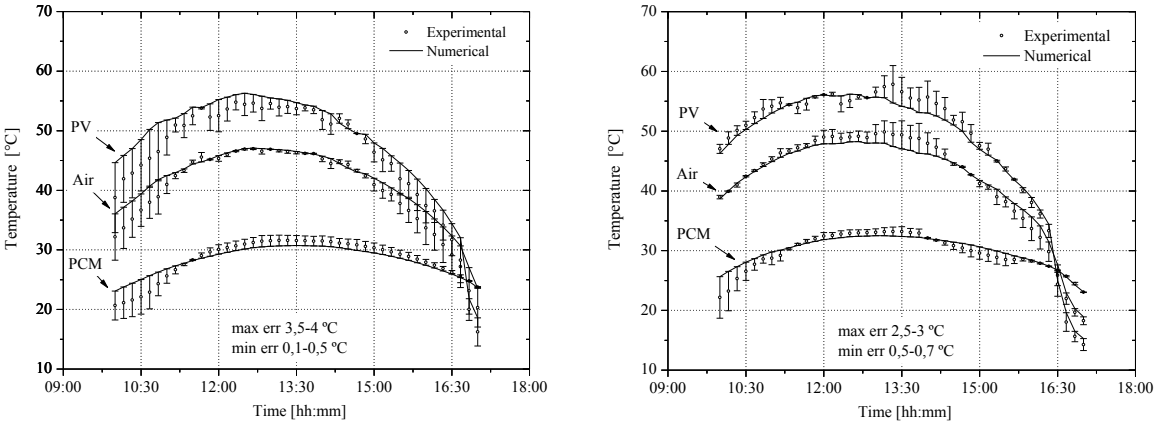

(a) (b)

Fig. 6. (a) 24th of February; (b) 25th of February

4.2. System performance

The evaluation of the overall system performance was conducted by means of total system efficiency (η_0) which is the sum of the thermal efficiency (η_t) and the electrical efficiency (η_e) [13]:

$$\eta_0 = \eta_t + \eta_e \tag{8}$$

The thermal efficiency (η_t) was calculated as a function of the heat gains into the room divided the solar radiation (G, W/m^2) multiplied by the area of the control volume (A, m^2). In ventilated cases the gain into the room are considered to calculated as the sum of the heat flux through the wall (Q_{int}, W) plus the air flow coming from air cavity to the interior room (Q_V, W) [14]:

$$\eta_t = \frac{Q_{\text{int}} + Q_V}{G \times A} \tag{9}$$

The energy conversion efficiency (η_e) of a solar panel is the percentage of the solar energy to which the panel is exposed that is converted into electrical energy. This is calculated by dividing a panel's power output (P, W) by the total incident solar radiation (G, W/m^2) and the surface area of the solar panel (A, m^2) [13]:

$$\eta_e = \frac{P}{G \times A} \tag{10}$$

The system performance is shown in Fig. 7 where the total system efficiency is plotted together with the thermal efficiency of the system as a function of the parameter (T_{in} - T_{out})/G, [m^2.◦C/W].

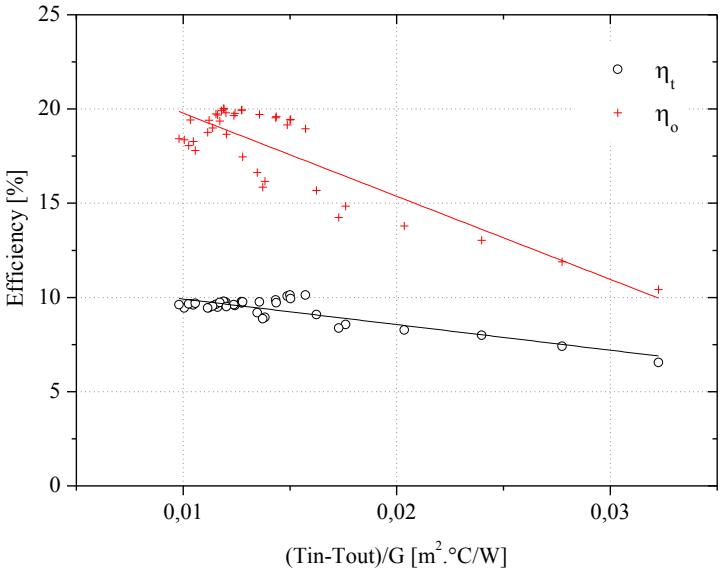

Fig. 7. Thermal and overall BIPV-PCM system efficiency

5. Conclusions

This paper reports the results of a preliminary study of an innovative building integrated system made of photovoltaic panels and phase-change thermal storage materials.

A simplified thermal network model for BIPV-PCM has been developed in MATLAB/SIMULINK® which allowed comparing the numerical results with experimental results obtained from testing the BIPV-PCM system after its installation on SolarXXI building façade. A comparison between simulated and experimental results in terms of temperature values has been performed and demonstrates that numerical model is able to predict the thermal behavior of the system with fairly good agreement with most discrepancies occurring when air flow begins to flow into the gap.

Regarding the system performance, the thermal and electric efficiencies calculated show a thermal system efficiency of about 10% and an overall system efficiency (electrical and thermal) of about 20%.

The future work is dedicated to the study of the performance of this system during cooling period and the optimization studies in order to improve the system performance towards accomplishment of the proposed objective of the project.

Acknowledgments

This work is part of a project PTDC/AURAQI-AQI/117782/2010 co-financed by FEDER.

References

[1] European Commission. Directive 2010/31/EU of the European Parliament and of the Council of 19 May 2010 on the energy performance of buildings. Official Journal of the European Union; 2010.

[2] Chen Y, Athienitis AK, Galal K. Modeling, Design and thermal performance of a BIPV/T system thermally coupled with a ventilated concrete slab in a low energy solar house: Part 1, BIPV/T system and house energy concept. Solar Energy 2010;84:1892–907.

[3] Szymocha K. Advanced thermal solar system with heat storage for residential house space heating. SESCI 2005 Conf., Burnaby: 2005, p. 1–10.

[4] Athienitis AK, Zhang J. A Study of Double Facades with Phase-Change Storage and Photovoltaics. Int. Conf. "Passive Low Cool. Built Environ., Department of Buildind, Civil and Environmental Engineering of Concordia University: 2005, p. 855–9.
[5] Bouzoukas A. New Approaches for Cooling Photovoltaic/Thermal (PV/T) Systems. University of Nottingham, 2008.
[6] Krauter S, Araújo RG, Schroer S, Hanitsch R, Salhi MJ, Triebel C, et al. Combined photovoltaic and solar thermal systems for facade integration and building insulation. Sol Energy 1999;67:239–48.
[7] Test FL, Lessmann RC, Johary A. Heat Transfer During Wind Flow over Rectangular Bodies in the Natural Environment. J Heat Transfer 1981;103:262.
[8] Duffie AJ, Beckman AW. Solar Engineering of Thermal Processes. 2nd ed. Jonh Wiley & Sons, INC; 1980.
[9] Kalogirou SA. Solar Energy Engineering - Processes and Systems. 1st ed. London: Elsevier; 2009.
[10] Jaber S, Ajib S. Optimum design of Trombe wall system in mediterranean region. Solar Energy 2011;85:1891–8.
[11] Santos CAP dos, Matias LMC. Coeficientes de Transmissão Térmica De Elementos da Envolvente do Edificios. 1st ed. Lisboa: LNEC; 2006.
[12] Athientis AK, Liu C, Hawes D, Banu D, Feldman D. Investigation of the thermal performance of a passive solar test-room with wall latent heat storage. Building Environment 1997;32:405–10.
[13] Chow TT. A review on photovoltaic/thermal hybrid solar technology. Applied Energy 2010;87:365–79.
[14] Lin Y, Chiang C, Lai C. Energy Efficiency and Ventilation Performance of Ventilated BIPV Walls. Engineering Application of Computational Fluid Mechanics 2011;5:479–86.